Supplementary information

for

Multi-spin-state at $Li_3PO_4/LiCoO_2$ (104) interface

Submitted by

Masato Sumita[†], Takahisa Ohno[†, ‡, ¶]

[†]National Institute for Materials Science (NIMS), 1-1 Namiki, Tsukuba, Ibaraki 305-0044, Japan, [‡]Global Research Center for Environment and Energy based on Nanomaterials Science (GREEN), NIMS, 1-1 Namiki, Tsukuba, Ibaraki 305-0044, Japan, [¶]Institute of Industrial Science, University of Tokyo, Meguro, Tokyo 153-8505, Japan

Contents:

1. Computational details

All calculations were performed with DFT implemented in CP2K.[S1] Total energies were calculated at the Γ point by a supercell approach. We used the PBE functional[S2] with the local spin density approximation (LSD). The hybrid Gaussian (MOLOPT DZVP) and plane-wave (500 Ry for cutoff energy) basis set,[S3] where valence pseudo-wavefunctions are expanded in Gaussian-type orbitals and the density is represented on a plane wave auxiliary basis, were used with the Goedecker, Teter, and Hutter (GTH) pseudopotentials[S4] constructed for the PBE functional. To include the electronic correlation within the d orbital of Co, we applied the +U strategy. The effective U was set to be 3.0 eV, as suggested in a previous research.[S5]

For DF-MD calculation, canonical sampling using velocity rescaling (CSVR) thermostat[S6] was used at a temperature of 400 K. Because no suitable density of amorphous Li_3PO_4 is known, we utilized an NPT ensemble under 1.0 atm, in which the cell parameter of the *c*-axis can be altered flexibly such that the density of the amorphous Li_3PO_4 is automatically adjusted to a suitable value. The time step was set to be 1.0 fs. After equilibration, trajectories that last more than 40.0 ps (40000 structures) were used for sampling.

2. Cell parameters of a $LiCoO_2$ (104) slab

To model a $Li_3PO_4/LiCoO_2$ (104) interface, we have employed a supercell geometry which is composed of a $LiCoO_2$ (104) slab and an amorphous Li_3PO_4 slab. For $LiCoO_2$, a cubic cell structure can be made from a rhombohedral structure with space group R3-m.[S7] The lattice vectors (that is, the *a*, *b*, and *c* axes) of the cubic $LiCoO_2$ correspond to the $[\bar{1}14]$, $[0\bar{1}4]$, and [104] directions of the original rhombohedral $LiCoO_2$, respectively. Therefore, a $LiCoO_2$ (104) slab can be constructed based on this cubic $LiCoO_2$ cell. Figure S1 shows a cubic $LiCoO_2$ cell, which includes 16 $LiCoO_2$ units. The cell parameters and the atom positions of the $LiCoO_2$ supercell were optimized through the geometry optimized algorithm. The optimized cell parameter is calculated to be 8.014 Å, respectively, which are in good agreement with the experimental value of 8.013 Å, which is estimated from the experimental cell parameter of the rhombohedral $LiCoO_2$ cell [S8]. We used the calculated cell parameter of 8.014 Å as the cell parameters of the *a* and *b* axes both for a $LiCoO_2$ (104) surface slab and a $Li_3PO_4/LiCoO_2$ interface.

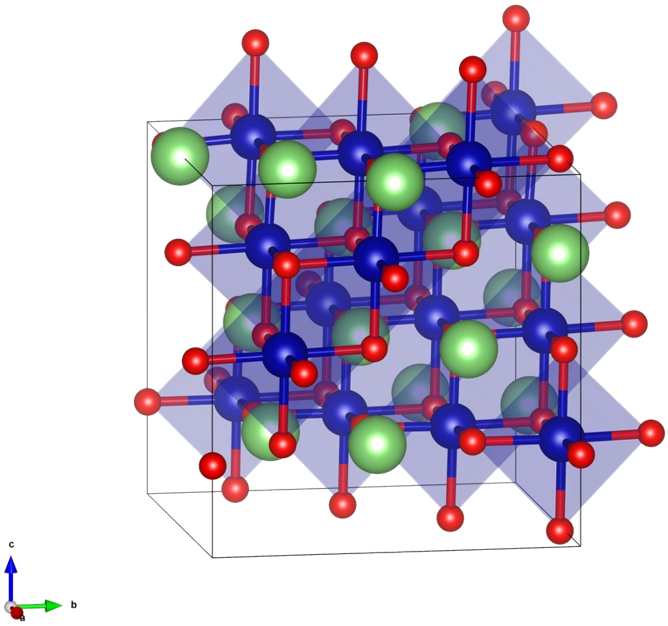

Figure S1. Cubic $LiCoO_2$ unit cell. We have optimized cell parameters and atom positions of the $LiCoO_2$ supercell. Obtained cell parameters are also used for a $LiCoO_2$ (104) surface slab calculation and a $Li_3PO_4/LiCoO_2$ (104) interface.

3. $LiCoO_2$ (104) surface

We have constructed a $LiCoO_2$ (104) surface slab based on the optimized cubic $LiCoO_2$ cell, which is composed of 28 $LiCoO_2$ units and includes seven Co layers, as shown in Figure S2. By using this slab geometry, we have calculated the energies of the $LiCoO_2$ (104) surfaces both with the IS Co atoms and with the LS Co atoms on the surface. In Table S1, we have summarized the energies of these two surfaces. The $LiCoO_2$ surface slab with the IS Co atoms is more stable than that with the LS Co atoms by 2.12 eV (0.26 eV / one Co atoms).

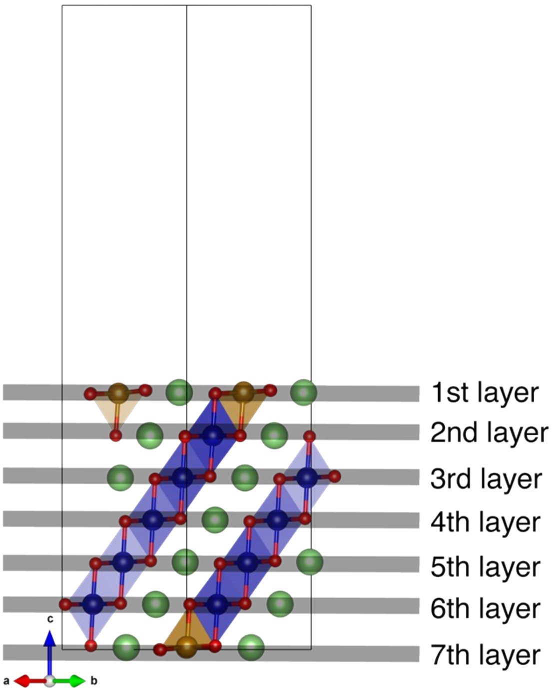

Figure S2. $LiCoO_2$ (104) surface slab with the 8.014×8.014×30.0 Å supercell. The Co layers ate numbered from 1st to 7th, where the 4th layer is the middle one.

Table S1. Energies of $LiCoO_2$ (104) surface with intermediate-spin (IS) Co and low-spin (LS) Co atoms on the surface.

	Intermediate	Low
Energy / Eh	-5180.110384	-5180.032545

Figures S3 and S4 show the layer density of states (LDOS) along the *c* axis of the $LiCoO_2$ (104) surface slab shown in Figure S2. Judging from that the LDOSs of the third and fifth layers are very similar to that of the fourth (middle) layer of the $LiCoO_2$ slab, the fourth layer can be regarded as the bulk region, where the band gap is estimated to be 2.3 eV.

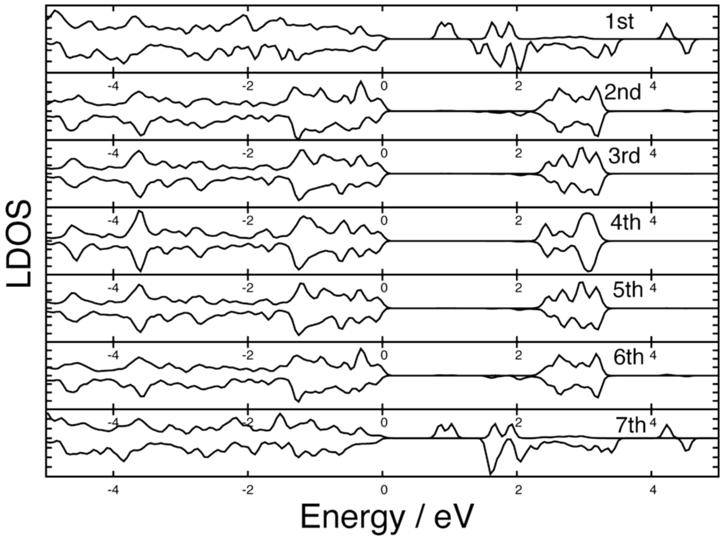

Figure S3. LDOS along the *c* axis of the $LiCoO_2$ (104) surface slab where Co_{5C} have the IS configuration. The first and seventh layers have interfacial states due to the existence of Co atoms which have the IS configuration.

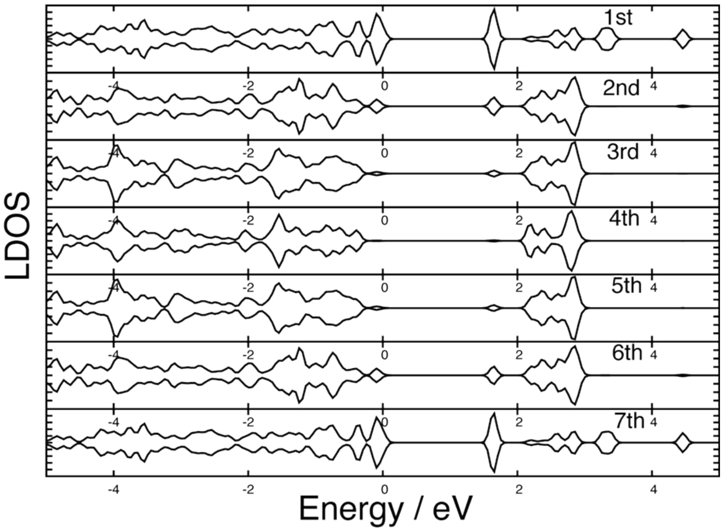

Figure S4. LDOS along the *c* axis of the $LiCoO_2$ (104) surface slab where all Co atoms have the LS configuration. The first and seventh layers have some interfacial levels.

4. Setup of an initial structure of the $Li_3PO_4/LiCoO_2$ (104) interface

We have constructed a $Li_3PO_4/LiCoO_2$ (104) supercell geometry which is composed of the $LiCoO_2$ (104) surface slab obtained in the above section S2 and an open space where an amorphous Li_3PO_4 slab is inserted afterwards. The cell parameter for the *c* axis (perpendicular to the interface) is initially set to be 50.0 Å. An amorphous Li_3PO_4 slab structure with randomly-distributed Li_3PO_4 units, whose lattice parameters in the directions parallel to the interface are adjusted to those of the $LiCoO_2$ (104) slab, is obtained as the following procedures:

(1) First, we have set up a (3×1×2) super cell of γ-Li_3PO_4[S9] using the calculated cell parameters. The *a'*, *b'*, and *c'* axes of the γ-Li_3PO_4 cell correspond, respectively, to the *c*, *b*, and *a* axes of the $Li_3PO_4/LiCoO_2$ (104) interface. The γ-Li_3PO_4 super cell includes 24 Li_3PO_4 units and the density is approximately 2.2 g/cm^3. To reduce the density a little bit, one Li_3PO_4 unit is removed from this super cell.

(2) Second, we have obtained an amorphous Li_3PO_4 structure at these cell parameters by performing DF-MD calculations at a high temperature of 1000 K under an NVT ensemble.

(3) Then, we have performed DF-MD calculations at 400 K under an NVT ensemble, by changing gradually the Li_3PO_4 cell parameters of the *b'* and *c'* axes into those of the *a* and *b* axes of the $LiCoO_2$ (104) slab, respectively, together with changing the cell parameter of the *a'* axis so as to keep the cell volume unchanged.

The amorphous Li_3PO_4 slab structure obtained through the above (1)-(3) procedures is inserted into an open space between the $LiCoO_2$ (104) slabs of the $Li_3PO_4/LiCoO_2$ (104) supercell such that any chemical bonds are not initially formed between the $LCoO_2$ and the Li_3PO_4 slabs. The obtained initial $Li_3PO_4/LiCoO_2$ interface structure is shown in Figure S5. The density of the amorphous Li_3PO_4 slab in this supercell is estimated to be approximately 1.98 g/cm^3. Starting from the obtained initial interface structure, we have performed DF-MD calculations with an NPT ensemble under 1.0 atm, in which the cell parameter of the *c*-axis can be altered flexibly such that the density of the amorphous Li_3PO_4 slab is automatically adjusted to a suitable value.

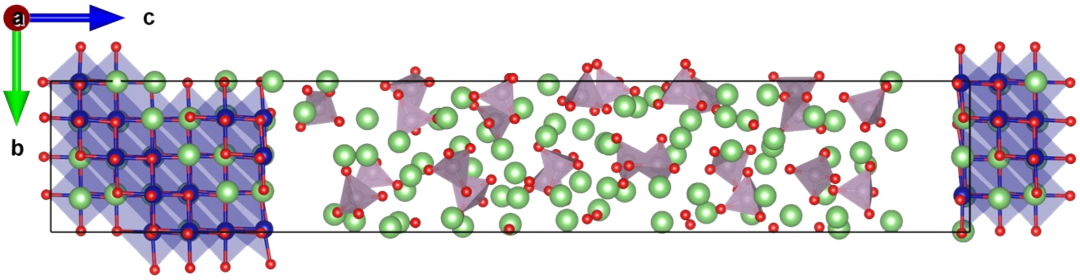

Figure S5. Initial structure of a Li_3PO_4/$LiCoO_2$ (104) interface in a supercell geometry. The cell parameter for the *c* axis is initially set to be 50.0 Å (that is flexibly altered in an NPT ensemble). The other cell parameters for the *a* and *b* axes are set to be those of the bulk $LiCoO_2$, i.e., 8.014 and 8.014 Å, respectively.

References

(S1) The CP2K developers group, http://www.cp2k.org/.

(S2) J. P. Perdew, K. Burke, M. Ernzerhor, *Phys. Rev. Lett.* 1996, **77**, 3865.

(S3) G. Lippert, J. Hutter, M. Parrinello, *Mol. Phys.* 1997, **92**, 477.

(S4) S. Goedecker, M. Teter, J. Hutter, *Phys. Rev. B*, 1996, **54**, 1703.

(S5) D. Qian, Y. Hinuma, H. Chen, Li. -S. Du, K. J. Carroll, G. Ceder, C. P.Grey, Y. S. Meng, *J. Am. Chem. Soc.* 2012, **134**, 6096.

(S6) G. Bussi, D. Donadio, M. Parrinello, *J. Chem. Phys.* 2007, ***126***, 014101(7 p).

(S7) K. Nishio, T. Ohnishi, K. Akatsuka, K. Takada, *J. Power Sources.* 2014, **347**, 687.

(S8) Q. Lin, Q. Li, K. E. Gray, J. F. Mitchell, *Crystal Growth & Design*, 2012, **12**, 1232.

(S9) J. Zemann, *Acta Crystallogr*. 1960, **13**, 863.